15th IFK
Proc. of the 15th International Fluid Power Conference <Symposium/Conference>
<DOI>

Analysis of Structure-Borne Noise Emissions of Axial Piston Pumps Using Blocked Forces and Virtual Point Transformation

Matthias Vogt[1,2,*] and Marcus Geimer[1]

[1]Institute of Mobile Machines (Mobima), Karlsruhe Institute of Technology (KIT), Karlsruhe, Germany
[2]Development of Axial Piston Units, Bosch Rexroth AG, Horb am Neckar, Germany
E-mail: matthias.vogt@partner.kit.edu; marcus.geimer@kit.edu
**Corresponding Author*

Abstract

With the shift towards electrification and the advancement of quieter internal combustion engines, the noise produced by axial piston pumps has gained increased attention. While fluid-borne noise emissions resulting from pulsating flow and airborne noise emissions through the housing of hydraulic pumps are well researched, studies on structure-borne noise emissions–transmitted to adjacent structures via the pump's mechanical mounting–are rare. One method to describe these emissions is through blocked forces, which allow for a receiver-independent characterization of structure-borne noise sources. In this publication, the excitation characteristics of an axial piston pump are analyzed based on blocked forces, which can be projected onto one or several points at the interface using the so-called virtual point transformation. The extent to which the pump's description differs when using one or two virtual points is investigated. The structure-borne noise excitation caused by the pump is examined during a speed run-up, allowing for the identification of dominant excitation degrees of freedom. It is indicated that for the axial piston pump under investigation, a source description utilizing a single virtual point is sufficient.

Keywords. Axial Piston Pumps, Structure Borne Noise, Blocked Forces, Virtual Point Transformation

1. INTRODUCTION

In addition to the airborne noise (ABN) directly emitted from the pump housing, hydraulic pumps also emit fluid-borne (FBN) and structure-borne noise (SBN) through the connection points into the overall system. Previous studies [1], [2], [3], [4], [5] indicate that these noise contributions have a significant impact on the overall sound power level of hydraulic systems. Fiebig [1] even states that hydraulic systems typically exhibit sound power levels that are 4 to 12 dB(A) higher than those of the pumps themselves, concluding that it is

unlikely that the ABN from the pumps housing constitutes the main sound power sources in such hydraulic systems.
While the excitation due to pressure pulsation is well-researched [6], [7] and established methods and standards [8], [9] for its determination exist, the SBN transmitted through the pump mounting points into the system remains largely unexplored. Fiebig's investigation [1] shows that this type of excitation can be a major cause of noise in hydraulic systems. In his study the dynamic forces generated by the pump are transmitted as SBN to the electric motor via the pump mounts. The motor and other large components act as noise radiators, converting this SBN energy into ABN. Therefore, knowing the pump emitted SBN at the interface also opens up various optimization potentials, such as optimizing the matching of excitation characteristics and system behavior through finite element simulation or designing decoupling elements between the pump and motor, as well as between the motor and the motor base.
A promising method to experimentally determine the SBN excitation at the pump mounting points independently of the receiver system is the "In situ Blocked Force Method" described in the ISO20270 standard [10], where the so-called blocked forces are used to characterize SBN sources. In [11], it has been demonstrated that this method can be successfully applied to an axial piston pump, thereby enabling the assessment of the SBN emission of hydraulic pumps.
In the following study, the source characterization based on experimentally determined blocked forces is further investigated. Therefore, the source description of an axial piston pump using one or two virtual contact points is compared. Furthermore, it is examined which excitation degree of freedom (DoF) are the most dominant for the investigated pump.

The publication is structured as follows: First, the theoretical foundations of the “Virtual Point Transformation” and “Component-based Transfer Path Analysis” are introduced. This is followed by a method for aggregating virtual point forces and torques into a single force and torque quantity. These concepts are then applied to an axial piston pump, and the results of the different methods are presented. Finally, the key insights are summarized, and an outlook on future work is provided.

2. METHODS

A fundamental prerequisite for analyzing SBN excitation from a hydraulic pump is the determination of quantities that describe the pump-induced SBN at the interface to a receiving system. Consequently, the following section introduces various concepts of transfer path analysis and source characterization.

2.1. Virtual Point Transformation

A critical aspect in the description of SBN sources is the definition of the interface between the source and the receiver system. Particularly when the excitation of a source is to be combined with the behavior of a passive receiver, the coupling points must be clearly defined. However, this is often not the case for quantities determined through measurement techniques, as source excitation and receiver behavior are measured in different ways or using different measurement setups.
One way to overcome this is the so-called Virtual Point Transformation (VPT). The concept was first introduced by van der Seijs et al. [12] and aims to project interface quantities (interface DoF) onto a set of interface displacement modes (IDMs), thereby enabling a clear

definition of the interface. When IDMs correspond to the six DoF (3 translational and 3 rotational) of a virtual point (VP), they are also known as rigid interface modes or virtual point DoF. A detailed description of the mathematical framework of the VPT is beyond the scope of this publication and has already been thoroughly described in various studies [12], [13], [14].

As the designation of the VP DoF as rigid interface modes implies, the classical VPT is based on the rigid body assumption. This means that the motions or forces projected onto a VP via VPT are assumed to behave as those of a rigid body. This condition can only be satisfied within a limited frequency range, depending on the structural dynamic behavior of the interface. In particular, the geometry and material properties of the interface significantly influence this range. If the rigid body condition is not fulfilled, the interface can no longer be fully described by the VP.

If a single VP is insufficient to describe the interface, as it is often the case for systems with multiple mounting points or flange-like contacts [15], [16], multiple VPs can be employed to represent the interface. The rigid body condition must then be satisfied only for each individual VP, thereby typically enabling the description of the source SBN excitation up to higher frequencies.

For the axial piston pump investigated, featuring a two-bolt mounting flange according to DIN ISO 3019-1 [17], two VPT setups were examined: one with a single VP (1VP setup) located at the center of the interface, and another with two VPs positioned at the mounting points (2VP setup). Figure 1 schematically illustrates both setups along with their respective interface DoF. While the 1VP setup requires only six DoF to describe the interface, the 2VP setup necessitates twelve DoF.

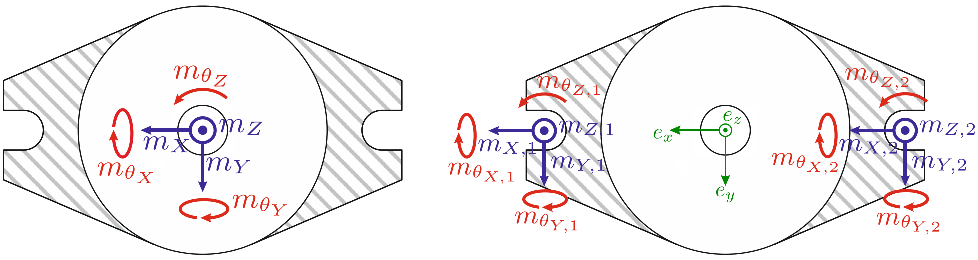

Figure 1: Schematic illustration of VPT setups for the axial piston pump. Left: 1VP setup with six DoF. Right: 2VP setup with twelve DoF.

2.2. Component-based Transfer Path Analysis

The primary objective of Transfer Path Analysis (TPA) is to identify the contributions of various noise sources and transmission paths to the overall noise level. A key step in TPA is source characterization, which aims to define a set of interface quantities that accurately describe the source's excitation at the interface with the passive receiving structure. Various interface quantities can be utilized for this purpose; however, for analyzing the source excitation itself, receiver-independent interface quantities are particularly valuable. When such quantities are used to describe the source, the TPA approach is referred to as component-based TPA (cTPA).[18]

The three most common methods of cTPA are illustrated in Figure 2. The “Free Velocity” method represents the extreme case where the source operates under freely vibrating conditions. In this scenario, the velocities measured at the interface $\mathbf{u}_2^{\text{free}}$ are independent of the receiver and thus represent a pure characteristic of the source. However, this method is unsuitable for hydraulic pumps, as a motor is required to drive the pump. The other extreme case is the “Direct Blocked Force” method, which assumes that the receiver connected to the source is infinitely stiff. Under this assumption, the forces measured at the interface, known as blocked forces $\mathbf{f}_2^{\mathrm{eq}}$, are independent of the receiver. Nonetheless, this method presents practical challenges, as detailed in [11].

A method that avoids such extreme boundary conditions is the “In Situ Blocked Force” method, which was first introduced by Moorhouse et al. [19]. Moorhouse et al. demonstrated that the blocked forces can also be determined in systems that are not infinitely stiff by applying a matrix inversion procedure. By means of this two-stage approach, the influence of the receiving system can be removed, enabling the determination of the receiver-independent blocked forces. This approach allows for the determination of blocked forces *in situ*, meaning within the typical application and is adaptable to various SBN sources. Consequently, it has gained prominence in recent years, particularly in the automotive industry, and has been standardized in ISO 20270 [10]. A detailed description of its application to an axial piston pump is provided in [11], [13].

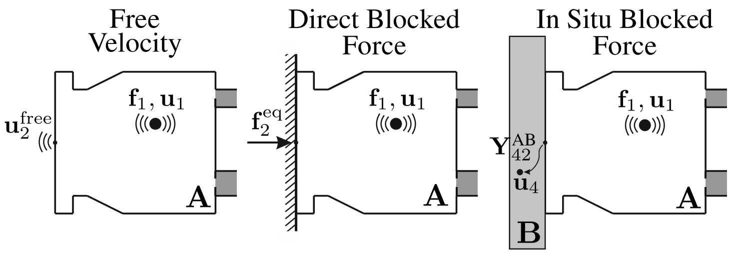

Figure 2: Common methods of source characterization in cTPA

The in situ blocked force method is based on the formula:

$$\mathbf{f}_2^{\mathrm{eq}} = (\mathbf{Y}_{42}^{\mathrm{AB}})^{+}\mathbf{u}_4 \tag{1}$$

which states that the blocked forces $\mathbf{f}_2^{\mathrm{eq}}$ can be determined by multiplying the vibration responses at the so-called indicator sensors $\mathbf{u}_4$ with the inverted transfer behavior $\mathbf{Y}_{42}^{\mathrm{AB}}$ from the interface to the indicators in the coupled state (denoted by $(\cdot)^{\mathrm{AB}}$). The symbol $(\cdot)^{+}$ denotes the pseudoinverse, as the transfer matrix $\mathbf{Y}_{42}^{\mathrm{AB}}$ is typically not a square matrix. From Equation 1, it follows that the method consists of two main steps:

Step 1: Determination of the transfer behavior $\mathbf{Y}_{42}^{\mathrm{AB}}$ from the interface to the indicators. This is typically achieved by exciting close to the interface using an impulse hammer or a shaker and measuring the vibration response at the indicators, usually with accelerometers.

Step 2: The source is in operation and the vibrations at the indicators $\mathbf{u}_4$ are measured. Using Equation 1, the blocked forces can then be calculated.

It is crucial to note that the blocked forces are determined exactly at the locations where the interface was excited with the impact hammer in Step 1. Because, in the in-situ blocked force method, the source and receiver are mechanically coupled, these excitation points are not located directly on the interface but rather in its vicinity, typically on the receiver structure. Consequently, the spatial positions of the blocked forces depend on the receiver geometry in the region around the interface, and the resulting blocked forces are therefore not completely receiver independent.

This receiver-dependency can be eliminated by transforming the blocked forces into VP coordinates, which are uniquely defined by the source itself. However, instead of transforming the blocked forces $\mathbf{f}_2^{\mathrm{eq}}$ into VP blocked forces and torques $\mathbf{m}_2^{\mathrm{eq}}$ after performing the in-situ blocked force TPA, it is also possible to transform the transfer matrix $\mathbf{Y}_{42}^{\mathrm{AB}}$ beforehand. The measured matrix is usually denoted $\mathbf{Y}_{42,\mathrm{uf}}^{\mathrm{AB}}$, where the subscripts $(\cdot)_{\mathrm{u}}$ and $(\cdot)_{\mathrm{f}}$ are added to indicate that this corresponds to the original form of the matrix. The transformed matrix is denoted $\mathbf{Y}_{42,\mathrm{um}}^{\mathrm{AB}}$, as only the forces are transformed into VP coordinates, whereas the measured motions at the indicator sensors are not transformed. This has the benefit that by transforming only the forces into VP coordinates, the number of force DoF is reduced, while the number of motion DoF remains constant. This results in a higher overdetermination of $\mathbf{Y}_{42,\mathrm{um}}^{\mathrm{AB}}$ compared to $\mathbf{Y}_{42,\mathrm{uf}}^{\mathrm{AB}}$, leading to a more stable matrix inversion. In the ISO 20270 standard an overdetermination by a factor between 2 and 3 is suggested. By applying the VPT exclusively to the forces, the recommended overdetermination factor can be achieved with smaller number of sensors to capture the vibrations $\mathbf{u}_4$.

It is important to note, that both matrices, $\mathbf{Y}_{42,\mathrm{uf}}^{\mathrm{AB}}$ and $\mathbf{Y}_{42,\mathrm{um}}^{\mathrm{AB}}$, represent the transfer behavior $\mathbf{Y}_{42}^{\mathrm{AB}}$ schematically shown in Figure 2. However, $\mathbf{Y}_{42,\mathrm{uf}}^{\mathrm{AB}}$ uses the original physical excitation points of the impact hammer or shaker, whereas $\mathbf{Y}_{42,\mathrm{um}}^{\mathrm{AB}}$ uses the VP DoF.

Using this, the relation for the in situ blocked force TPA becomes

$$\mathbf{m}_2^{\mathrm{eq}} = (\mathbf{Y}_{42,\mathrm{um}}^{\mathrm{AB}})^{+}\mathbf{u}_4, \tag{2}$$

which allows for the determination of the blocked forces directly in the VP coordinates.

An additional benefit of the in situ blocked force method is that it allows for direct validation of the source description through the blocked forces. This validation step is referred to as On-Board Validation (OBV). For this purpose, additional validation sensors $\mathbf{u}_3$ are located on the receiver, which are not used for determining the blocked forces. The transfer behavior $\mathbf{Y}_{32,\mathrm{uf}}^{\mathrm{AB}}$ can be directly determined during the measurement of $\mathbf{Y}_{42,\mathrm{uf}}^{\mathrm{AB}}$, resulting in minimal additional effort. After the blocked forces have been determined using Equation 2, the movement at the validation points $\mathbf{u}_3$ can be predicted using the blocked forces through the relationship

$$\mathbf{u}_3^{pred.} = \mathbf{Y}_{32,\mathrm{um}}^{\mathrm{AB}}\mathbf{m}_2^{\mathrm{eq}}. \tag{3}$$

These predicted motions can then be compared with the directly measured signals $\mathbf{u}_3^{meas.}$, providing an initial validation of the blocked forces. If the blocked forces are unable to describe the excitation by the source, or if numerical errors occur during the inversion of the matrix $\mathbf{Y}_{42,\mathrm{um}}^{\mathrm{AB}}$, this will be evident in the OBV.

2.3. Aggregation of Blocked Forces and Blocked Torques Using Vector Norms

As already explained in [13], blocked forces and torques can be summarized using the vector norm, which is particularly useful when the goal is a straightforward evaluation of a SBN source. Here, the aggregation of blocked forces and torques is specifically used to analyze whether the source description with two VPs is advantageous or if a single VP is sufficient. For the single VP case, the procedure is identical to that in [13], and the force or torque vector norm is determined as follows:

$$\|\mathbf{F}_{1VP}\| = \sqrt{{F_x}^2 + {F_y}^2 + {F_z}^2} \tag{4}$$

$$\|\mathbf{M}_{1VP}\| = \sqrt{{M_x}^2 + {M_y}^2 + {M_z}^2} \tag{5}$$

In contrast, the 2VP setup introduces additional complexity because not all six force and torque components can be directly combined using vector norms without distinguishing between the two VPs. Moreover, the coupling between the two VPs must be taken into account: unlike in the single-VP case—where only one VP emits vibration power—the two-VP setup also involves power exchange between the VPs.

In general, for SBN sources described by multiple contact points or VPs, two special cases may occur. The first case arises when the VPs are not coupled, i.e., they behave completely independently. This condition is analogous to neglecting transfer-mobilities between coupling points in a power-based approaches. Previous investigations have shown that this simplification can be valid, for example, in systems with multiple point contacts that are connected to the receiver via resilient mounts [20]. In such cases, it is reasonable to treat the two VPs as separate sources. However, if the primary goal is to minimize the number of evaluation quantities, energetic aggregation of all force and torque components of the two VPs can also be considered. However, for the investigated axial piston pump, this first case is likely less relevant. Instead, it can be assumed that the pump's steel flange behaves like a rigid body over a broad frequency range, leading to strong coupling between the two VPs in the 2VP setup.

The second special case, which is therefore more plausible for the investigated axial piston pump, is that the VPs of a SBN source behave like points of a rigid body. In this case, the forces and torques of the two VPs can be geometrically combined into a total force and a total torque as follows:

$$\mathbf{F}_{2VP} = \mathbf{F}_{VP1} + \mathbf{F}_{VP2} \tag{6}$$

$$\mathbf{M}_{2VP} = \mathbf{M}_{VP1} + \mathbf{M}_{VP2} + \mathbf{r}_{VP1} \times \mathbf{F}_{VP1} + \mathbf{r}_{VP2} \times \mathbf{F}_{VP2} \tag{7}$$

Assuming rigid-body behavior is fully satisfied, these quantities are coherently combined in phase. Subsequently, the vector norms of the resulting force vector $\|\mathbf{F}_{2VP}\|$ and the resulting torque vector $\|\mathbf{M}_{2VP}\|$ can be calculated similarly to the 1VP setup. A key point is that the total torque in Equation 7 introduces terms of the form $\mathbf{r} \times \mathbf{F}$, which represent torques arising from the rigid coupling of the VPs [21]. The vectors $\mathbf{r}$ denote the relative vectors from a reference point to each respective VP. For later comparison with the single VP setup, the position of the sole VP in the 1VP setup can be chosen as the reference point. Provided that the interface behaves as a rigid body, the norms $\|\mathbf{F}_{1VP}\|$, $\|\mathbf{M}_{1VP}\|$, and $\|\mathbf{F}_{2VP}\|$, $\|\mathbf{M}_{2VP}\|$, should then be identical. However, it is evident that this method of combining forces and torques of the 2VP setup negates the primary advantage of describing the source with two VPs, which is to require the rigid body condition to be fulfilled for only one VP.

When neither of the two special cases—independence between the individual virtual points or fulfilment of the rigid-body condition—is met, a straightforward aggregation of the SBN excitation on a force or torque level is not possible. Instead, extended approaches, such as power-based methods, must be applied [22].

For the following investigation of the axial piston pump, the aggregation of the 2VP setup under the assumption of rigid-body conditions is used to assess whether a description with two VPs is necessary, or if a single VP is sufficient.

3. RESULTS

In the following section, the results of the concepts introduced earlier will be presented, with a particular focus on comparing the 1VP and 2VP setups. It is important to note that all transfer functions, also called Frequency Response Functions (FRFs), were obtained through excitation with a shaker. This excitation method allowed for a sufficient signal-to-noise ratio to be achieved starting from 140 Hz. Consequently, all subsequent frequency-dependent quantities will be presented only for frequencies greater than 140 Hz. This lower frequency limit is sufficient to characterize the SBN of 9-piston axial piston pumps at rotational speeds of approximately 1000 rpm and higher, as the first harmonic at 1000 rpm occurs at 150 Hz. The upper considered frequency is 5 kHz, as this frequency is cited in the literature as the upper threshold for acoustic analysis of axial piston pumps [23].
All the results shown in the following were obtained with the support of the open-source Python package pyFBS [24], [25].

3.1. Virtual Point Transformation Quality

A straightforward method for analyzing the quality of the VPT is through the "Consistency" criterion. This metric assesses how accurately the measured forces or motions can be represented by the corresponding VP forces and motions. To determine the consistency, the measured transfer matrix is first transformed into VP coordinates and then mapped back to the original coordinates using the inverse VPT. If the rigid-body condition is fully satisfied, the reconstructed transfer matrix will match the originally measured matrix. However, if the rigid-body condition is violated, the reconstructed matrix will only contain the rigid-body motion, while the flexible dynamics are filtered out. Comparing the original and reconstructed matrices therefore serves as a quality indicator for how well the rigid-body assumption is fulfilled.
A detailed description of the consistency calculation is omitted here, as it would require a full introduction to the VPT, which is beyond the scope of this publication. The procedure is explained in [15], where it is also shown how, based on the original and reconstructed matrices, a single scalar value can be derived for impacts and sensors, using the vector norm. These values are referred to as overall sensor consistency and overall impact consistency, respectively.
In the following, the focus is on impact consistency, as the VPT is applied solely to the forces, as previously mentioned. The overall impact consistency for the 1VP and 2VP setups is illustrated in Figure 3. As demonstrated, the impact consistency for both setups remains approximately 100 % up to around 4.3 kHz. Beyond this frequency, the impact consistency of the 1VP setup declines sharply, whereas that of the 2VP setup remains high. According to these results, it can be concluded that the rigid body condition is satisfied for the 1VP setup only up to 4.3 kHz. For frequencies exceeding 4.3 kHz, the utilization of two VPs in the interface description provides a distinct advantage in impact consistency.
However, the determination of consistency is based solely on the measured transfer matrices and the geometric properties of the VPT. It does not allow for an assessment of whether the rigid body condition is also met during operation.

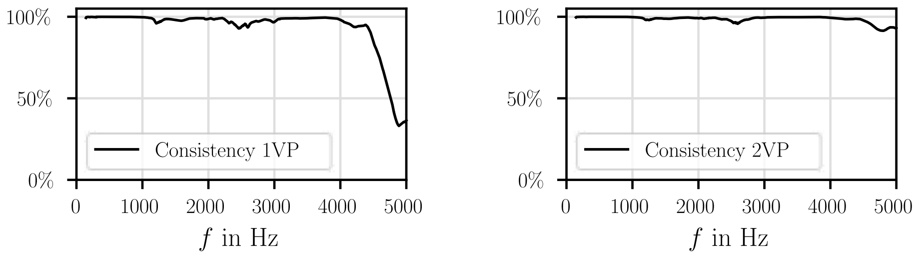

Figure 3: Overall impact consistency. Left: 1VP setup. Right: 2VP setup.

3.2. Results Stationary Operating Point

In the next step, the SBN excitation of an axial piston pump at a stationary operating point will be examined. Specifically, the operating point at $n = 2000$ rpm, $p = 200$ bar, and the maximum displacement volume $V_d = V_{d,max}$ will be considered. The pump investigated in the following study is suitable for use in a 6-ton mini excavator.

Figure 4 presents the results of the OBV for the 1VP and 2VP setups. In each case, the velocity measured directly at the validation sensors $\mathbf{u}_3^{meas.}$ is compared with the velocities predicted based on the blocked forces $\mathbf{u}_3^{pred.}$. The displayed velocity represents the vector norm of the three sensor channels of a triaxial accelerometer. A reference value of $v_{ref} = 10^{-6}$ m/s is used to calculate the dB value. Circles and crosses at the peaks of the harmonics were used to highlight the agreement at those frequencies.

It can be observed that both setups yield very similar results up to the 8th harmonic, i.e., 2.4 kHz, and that the direct measurements agree closely with the predictions within this frequency range. For the 1VP setup, the predictions become less accurate at certain higher harmonics, whereas for the 2VP setup, the predictions and measurements show good agreement, except at the 11th harmonic. Overall, it can be concluded that for both setups, the blocked forces and torques are capable of describing the SBN excitation of the axial piston pump, with the 2VP setup providing slightly better results for frequencies above 2.4 kHz.

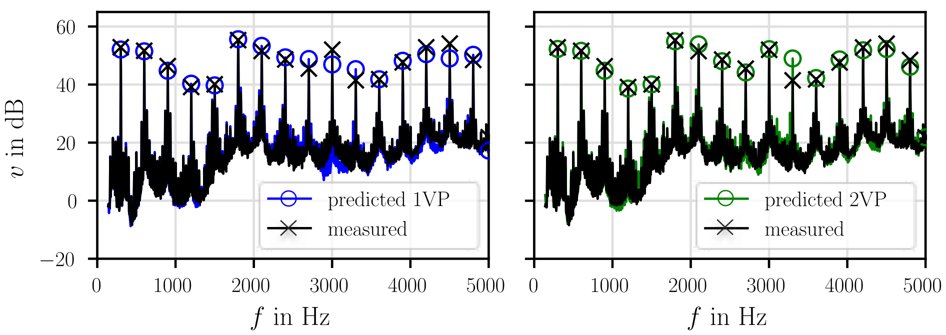

Figure 4: OBV for a stationary operating point. Left: 1VP setup. Right: 2VP setup.

The OBV method enables evaluation of whether interface quantities can describe the excitation caused by a SBN source. The primary objective of this study, however, is to quantitatively investigate the SBN excitation caused by the axial piston pump. Therefore, in the following the blocked forces and torques will be examined. Figure 5 presents the

aggregated blocked forces $\|\mathbf{F}\|$ and blocked torques $\|\mathbf{M}\|$ at the same operating point as the OBV, for both VP setups. For the calculation of the dB values a reference value of $F_{ref} = 10^{-6}$ N is used for forces and $M_{ref} = 10^{-6}$ Nm for Torques.
Before comparing the curves, it is important to first comprehend the differences in the vector norms between the two setups. In the 1VP setup, rigid-body behavior of the entire interface is assumed from the outset, and blocked forces and torques are determined under this assumption. The vector norms are then simply computed using Equations 4 and 5. In contrast, for the 2VP setup, blocked forces and torques are calculated under the condition that rigid-body behavior is satisfied for each VP individually, but not necessarily for the entire interface. The rigid-body assumption between the two VPs—and thus for the full interface—is only imposed later, when the forces and torques from the two VPs are aggregated using Equations 6 and 7.
Consequently, if $\|\mathbf{F}\|$ and $\|\mathbf{M}\|$ of the 1VP and 2VP setups agree, the rigid-body assumption must hold true during the aggregation of the 2VP setup via the vector norms, and thus also for the entire interface. Alternatively, if rigid-body assumption does not hold true, applying Equations (6) and (7) would be expected to produce discrepancies between $\|\mathbf{F}_{1VP}\|$ and $\|\mathbf{F}_{2VP}\|$ as well as $\|\mathbf{M}_{1VP}\|$ and $\|\mathbf{M}_{2VP}\|$. Therefore, the comparison of the vector norms between the two setups serves as a qualitative indicator of whether the rigid-body assumption is satisfied during operation.

Figure 5 shows that both $\|\mathbf{F}\|$ and $\|\mathbf{M}\|$ agree almost perfectly between the setups, with only minor deviations. This confirms what was already suggested by the evaluation of the impact consistency, namely that the interface behaves like a rigid body over a wide frequency range. However, it is interesting to note that while the consistency for the 1VP setup declines beyond 4.3 kHz, the determined vector norms still show good agreement at higher frequencies. This is likely because the consistency criterion is significantly more sensitive to violations of the rigid-body condition than the qualitative comparison of the norms. Yet, for the analysis of SBN excitation, the blocked forces and torques are of primary relevance, and these agree well for both setups. As a result, the considerably more complex interface description using two virtual points is not necessary, particularly as the dominant harmonics lie in the low-frequency range, where agreement is strongest.

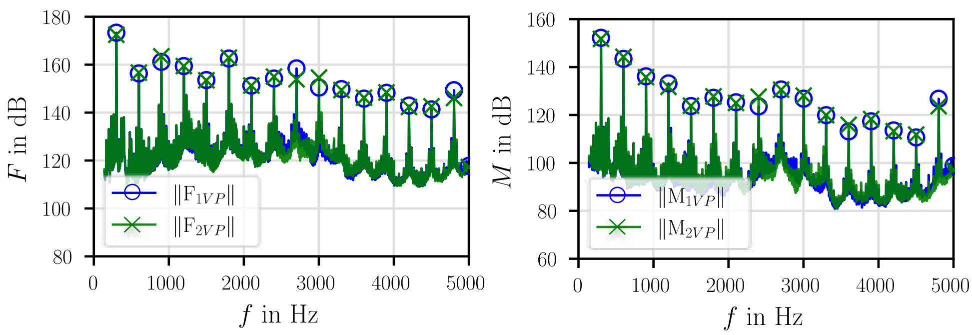

Figure 5: Comparison of SBN excitation for the 1VP and 2VP setup for a stationary operating point. Left: Norm blocked forces $\|\mathbf{F}\|$. Right: Norm blocked torques $\|\mathbf{M}\|$

3.3. Results Run-Up

As the final part of the analysis, the excitation of the SBN caused by the axial pistons during a speed run-up at a pressure of $p = 200$ bar and maximum displacement volume $V_d = V_{d,max}$ is examined. For each discrete speed step, a distinct excitation spectrum is obtained. Since analyzing each individual spectrum in detail would not be efficient, the spectra are consolidated by calculating the root-mean-square (RMS) value of each spectrum. The entire frequency range from 140 to 5000 Hz is considered in this calculation. However, as shown in Figure 5, it is expected that the resulting RMS value is primarily determined by the dominant low-frequency harmonics.

The corresponding blocked forces and blocked torques in each spatial direction are presented in Figure 6. Specifically, both the forces and torques of the 1VP setup $F_{i,1VP}$, $M_{i,1VP}$ and the total forces and torques per coordinate direction for the 2VP setup $\sum F_{i,2VP}$ $\sum M_{i,2VP}$ are shown. These results match almost perfectly, except for minor deviations in the torque around the z-axis, confirming the findings of the previous analysis.

For torques, the sum of the 2VP torques is additionally plotted with dotted lines, excluding the $\mathbf{r} \times \mathbf{F}$ terms of Equation 7. As expected, this omission has no effect on the torque in the x-direction $\sum M_{X,2VP}$, because the two VPs in the 2VP setup are displaced only along the x-direction (see Figure 1). However, for the other two directions, the torque is significantly underestimated when the $\mathbf{r} \times \mathbf{F}$ terms are omitted. This highlights the strong coupling between the two VPs and emphasizes that these terms must generally be taken into account when aggregating the torques of SBN sources described with multiple connection points.

Each plot also shows the vector norm of the 1VP forces $\|\mathbf{F}_{1VP}\|$ and torques $\|\mathbf{M}_{1VP}\|$. The vector norms of the 2VP setup are not shown, as they are nearly identical. This representation makes the dominant force or torque contribution at each rotational speed immediately visible, aiding in root-cause analysis and the development of countermeasures at critical operating points. If a critical operating point is identified, a detailed spectral analysis can help to determine harmonics responsible for strong SBN excitation.

For the axial piston pump under investigation, a key observation is that the force excitation is primarily dominated by the force in the y-direction, while the force in the z-direction contributes minimally to the overall excitation. Analysis of torque excitation revealed that all three rotational DoF significantly contribute to the overall excitation, depending on the rotational speed. For example, at 1500 rpm, the excitation is predominantly governed by torque around the z-axis, corresponding to axial torque excitation.

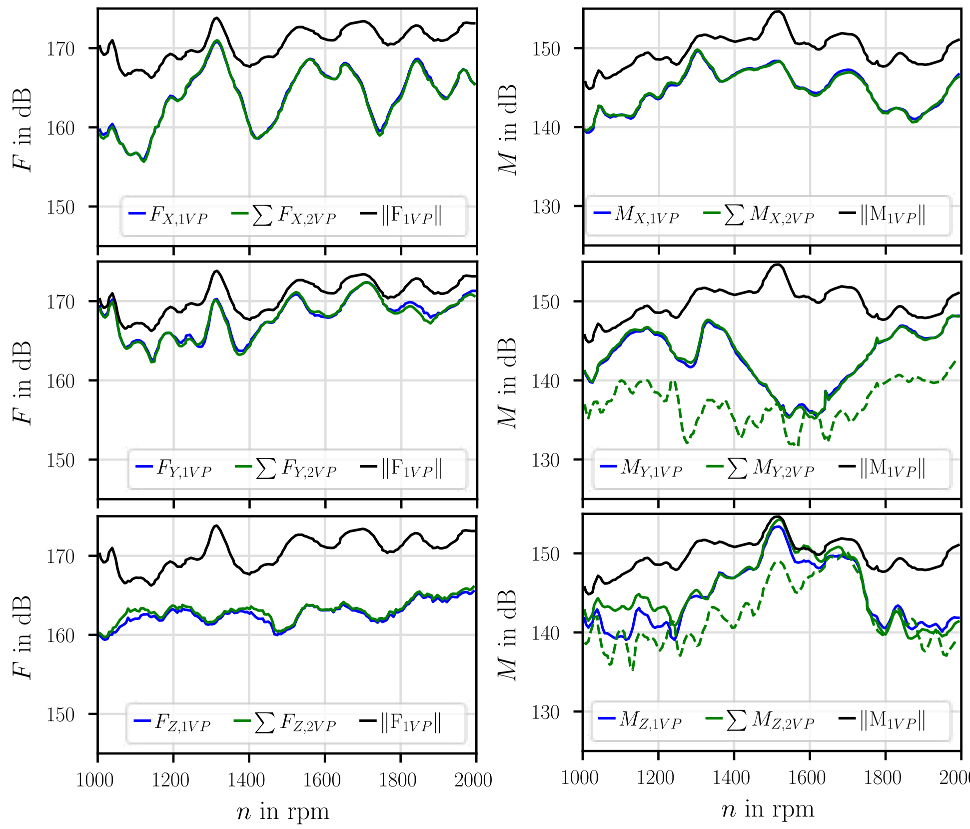

Figure 6: SBN excitation of an axial piston pump for a run-up. Left: Blocked forces. Right: Blocked torques (—— with $\mathbf{r} \times \mathbf{F}$ terms, - - - without $\mathbf{r} \times \mathbf{F}$ terms)

4. CONCLUSION AND OUTLOOK

To analyze the SBN excitation generated by an axial piston pump, the concepts of VPT and the in-situ blocked force TPA were introduced. For the investigated pump, a key objective was to compare the interface description of the pump using one versus two VPs.

Theoretical considerations indicate that that aggregating the interface forces and torques of multiple VPs using the vector norm is reasonable only when the VPs are largely independent or when the rigid-body assumption holds. In the latter case, however, it may be more appropriate to model the interface with a single VP from the outset.

This was also the case for the examined axial piston pump. When investigating the difference between the 1VP and 2VP setups, it was found that the coupling between the two VPs in the 2VP setup was very strong. Within the investigated frequency range, their interaction could be approximated as rigid body coupling. Consequently, representing the source with two VPs is unnecessary, and a single-VP representation in the center of the interface is more appropriate. However, it is important to note that this conclusion applies specifically to the pump under investigation and to the analysis of SBN excitation. As the OBV results show, describing an SBN source with multiple VPs can be advantageous—or even necessary—especially at higher frequencies.

Based on the blocked forces determined for a single VP, the SBN excitation of the pump can be analyzed for the individual DoF of the VP, enabling the identification and investigation of critical operating points. For the examined pump force excitation is predominantly in the y-direction, with minimal excitation in the z-direction. In contrast, for torque excitation, all directions contribute to the overall excitation, depending on the rotational speed of the pump.

A limitation of the applied approach is that forces and torques are evaluated separately and cannot be combined directly due to their differing physical units. A solution to this is provided by power-based approaches. By combining forces and torques with the corresponding velocities and angular velocities, power quantities for each DoF can be derived. This would allow for direct comparison between translational and rotational excitation.

Another promising direction is to study excitation in conjunction with a specific target system. Such an analysis would make it possible to evaluate which excitation DoF has the greatest influence on a specific target, like a microphone at the diver's ear, providing a more application-oriented understanding of the SBN.

5. ACKNOWLEDGEMENTS

Acknowledgements are given to Bosch Rexroth AG for the financial support and the provision of the acoustic test bench, as well as to the Bosch Sound Propagation expert team for their technical and professional support.

6. REFERENCES

[1] W. Fiebig, "Geraeuschminderung in hydraulischen Systemen," VDI Verlag, Düsseldorf, Germany, 337, 2008.

[2] R. Klop, "Investigation of Hydraulic Transmission Noise Sources," Purdue University, West Lafayette, IN, USA, 2010.

[3] R. Klop and M. Ivantysynova, "Investigation of Noise Sources on a Series Hybrid Transmission," *Int. J. Fluid Power*, vol. 12, no. 3, pp. 17–30, Jan. 2011, doi: 10.1080/14399776.2011.10781034.

[4] A. Waitschat, L. Nordmann, F. Thielecke, and V. Pommier-Budinger, "Enhanced Toolbox for the Combined Analysis of Fluid- and Structure-Borne Noise of Hydraulic Systems," in *BATH/ASME 2016 Symposium on Fluid Power and Motion Control*, Bath, UK: American Society of Mechanical Engineers, Sep. 2016, p. V001T01A001. doi: 10.1115/FPMC2016-1701.

[5] T. Opperwall and A. Vacca, "A Transfer Path Approach for Experimentally Determining the Noise Impact of Hydraulic Components," presented at the SAE 2015 Commercial Vehicle Engineering Congress, 2015, pp. 2015-01–2854. doi: 10.4271/2015-01-2854.

[6] T. Nafz, "Aktive Ventilumsteuerung von Axialkolbenpumpen zur Geräuschreduktion hydraulischer Anlagen," RWTH Aachen, Aachen, Germany, 2011.

[7] B. Müller, “Einsatz der Simulation zur Pulsations- und Geräuschminderung hydraulischer Anlagen,” RWTH Aachen, Aachen, Germany, 2002.

[8] International Organization for Standardization, *ISO 10767-1:2015 Hydraulic fluid power - Determination of pressure ripple levels generated in systems and components - Part 1: Method for determining source flow ripple and source impedance of pumps*, ISO 10767-1, 2015.

[9] International Organization for Standardization, *ISO 10767-1:1996 Hydraulic fluid power - Determination of pressure ripple levels generated in systems and components - Part 1: Precision method for pumps*, 1996.

[10] International Organization for Standardization, *ISO 20270-1:2019 Acoustics — Characterization of sources of structure-borne sound and vibration — Indirect measurement of blocked forces*, 2019.

[11] M. Vogt and M. Geimer, “An Approach for Evaluating Structure-Borne Noise Emission of Axial Piston Units Using Blocked Forces,” in *Proceedings of the 19th Scandinavian International Conference on Fluid Power (SICFP’25)*, Linköping, Sweden, 2025. doi: 10.13052/rp-9788743808251A35.

[12] M. van der Seijs, D. van den Bosch, D. Rixen, and D. de Klerk, “An improved methodology for the virtual point transformation of measured frequency response functions in dynamic substructuring,” in *Proceedings of COMPDYN 2013*, Kos Island, Greece, 2013, pp. 4334–4347. doi: 10.7712/120113.4816.C1539.

[13] M. Vogt and M. Geimer, “Comparison of different approaches for Evaluating Structure-Borne Noise Emission of Axial Piston Units,” in *Proceedings of DAGA 2025 (Deutsche Jahrestagung für Akustik)*, Copenhagen, Denmark, 2025.

[14] T. Bregar, A. El Mahmoudi, G. Čepon, D. J. Rixen, and M. Boltežar, “Performance of the Expanded Virtual Point Transformation on a Complex Test Structure,” *Exp. Tech.*, vol. 45, no. 1, pp. 83–93, Feb. 2021, doi: 10.1007/s40799-020-00398-1.

[15] M. V. van der Seijs, “Experimental Dynamic Substructuring: Analysis and Design Strategies for Vehicle Development,” Delft University of Technology, Delft, The Netherlands, 2016. doi: 10.4233/UUID:28B31294-8D53-49EB-B108-284B63EDF670.

[16] C. L. Balogh, T. Kimpián, and T. Ungvári, “An Examination of Component-Based TPA Performance and Feasibility for Steering Motors,” *J. Phys. Conf. Ser.*, vol. 2677, no. 1, p. 012011, Dec. 2023, doi: 10.1088/1742-6596/2677/1/012011.

[17] International Organization for Standardization, *ISO 3019--1:2001 Hydraulic fluid power - Dimensions and identification code for mounting flanges and shaft ends of displacement pumps and motors - Part 1: Inch series shown in metric units*, 2001.

[18] M. V. van der Seijs, D. de Klerk, and D. J. Rixen, “General framework for transfer path analysis: History, theory and classification of techniques,” *Mech. Syst. Signal Process.*, vol. 68–69, pp. 217–244, Feb. 2016, doi: 10.1016/j.ymssp.2015.08.004.

[19] A. T. Moorhouse, A. S. Elliott, and T. A. Evans, “In situ measurement of the blocked force of structure-borne sound sources,” *J. Sound Vib.*, vol. 325, no. 4–5, pp. 679–685, Sep. 2009, doi: 10.1016/j.jsv.2009.04.035.

[20] B. M. Gibbs and M. Villot, “Structure-borne sound in buildings: Advances in measurement and prediction methods,” *Noise Control Eng. J.*, vol. 68, no. 1, pp. 1–20, Jan. 2020, doi: 10.3397/1/37681.

[21] J. L. Meriam, J. N. Bolton, and J. L. /Kraige Meriam L. G., *Engineering Mechanics*, 9th ed. 2018.

[22] A. T. Moorhouse, “On the characteristic power of structure-borne sound sources,” *J. Sound Vib.*, vol. 248, no. 3, pp. 441–459, Nov. 2001, doi: 10.1006/jsvi.2001.3797.

[23] H. Münch, “Acoustically extended virtualization of industrial productsAkustisch erweiterte Virtualisierung von Industrieprodukten,” FAU Erlangen-Nürnberg, Erlangen, Germany, 2021. Accessed: Nov. 09, 2024. [Online]. Available: https://open.fau.de/handle/openfau/15906

[24] T. Bregar, A. El Mahmoudi, M. Kodrič, G. Čepon, M. Boltežar, and D. J. Rixen, “Introducing pyFBS: An Open-Source Python Package for Frequency Based Substructuring and Transfer Path Analysis,” in *Proceedings of the 39th International Modal Analysis Conference (IMAC XXXIX)*, M. S. Allen, W. D’Ambrogio, and D. Roettgen, Eds., 2021, pp. 81–89. doi: 10.1007/978-3-030-75910-0_10.

[25] T. Bregar *et al.*, “pyFBS: A Python package for Frequency Based Substructuring,” *J. Open Source Softw.*, vol. 7, no. 69, p. 3399, Jan. 2022, doi: 10.21105/joss.03399.

Biographies

Matthias Vogt received his B.Sc. (2019) and M.Sc. (2021) in Mechanical Engineering from the Karlsruhe Institute of Technology (KIT). From 2022 to 2023, he was a researcher at the Institute of Mobile Machines (Mobima) at KIT. Since 2023, he has been pursuing a Ph.D. at Mobima in cooperation with Bosch Rexroth AG. His research focuses on developing a method for evaluating the structure-borne noise emissions of axial piston pumps.

Marcus Geimer received his Diploma degree in mechanical engineering from the RWTH Aachen University, Aachen, Germany in 1990. In 1995, he received his Ph.D. from the Institute of Hydraulics and Pneumatics, today named Institute for Fluid Power Drives and Systems, RWTH Aachen University. He started his industrial career in 1995 in the field of construction at the company Krupp Berco Bautechnik GmbH, Essen (Germany). There, he was the leader of the research group for hydraulic breakers. In 2000, he changed to Bucher Hydraulics Gmbh, Klettgau (Germany), where he led the construction and customer development for mobile hydraulics. Since 2005, he is a full professor and director at the Institute of Mobile Machines (Mobima), at the Karlsruhe Institute of Technology KIT, Germany. Hydraulic and electric drives for the traction drive as well as for the working functions and controls for mobile machines are main research areas of the institute.